Modeling of the Axial Movement of Parts During Centerless Through-Feed Grinding

Kang Kim*

School of Mechanical and Automotive Engineering, Kookmin University, 861-1 Jungreung-dong, Sungbook-gu, Seoul 136-702, Korea

There are two major differences between the centerless infeed grinding process and the centerless through-feed grinding process. One is an axial movement of workpieces, and the other is that several workpieces are ground simultaneously and continuously by through-feeding. Because of these differences, through-feed ground parts inherently possess not only the roundness error but also the tapering error. The aims of the research reported in this paper are to examine this inherent tapering characteristic and to find the effects of grinding variables (center height angle, regulating wheel tilt angle, and shape of grinding wheel surface). To accomplish the objectives, experiments were carried out using two types of cylindrical workpiece shapes. Also, computer simulations were performed using the 3-D through-feed grinding model.

Key Words : Centerless Through-feed Grinding, Axial Motion of Workpiece, Tapering Error, Cylindricity, Global Deflection

1. Introduction

Although the centerless through-feed grinding process has been the most accurate and popular process for machining cylindrical parts, geometric characteristics of through-feed ground parts are not known well. The theoretical and experimental researches about geometric characteristics of in-feed ground part were presented by Dall (1946), Yonetsu (1959a, 1959b), and by Rowe and Barash (1964, 1965). They investigated the effects of centerless grinding variables on the out-of-roundness of the ground part. The researches on the through-feed process were also done by Yonetsu (1960) and Meis (1980). The results of these researches have been effective in controlling the roundness profiles of the parts. However, they are insufficient to reveal the cylindrical characteristics of through-feed ground parts three dimensionally.

The geometric tolerance defining the surface of a cylindrical part is cylindricity, which incorporates roundness, straightness and parallelism (taper) simultaneously. Because of the difficulty in measuring cylindricity, however, the roundness, straightness and parallelism (taper) tolerances are still used separately in a production line. With the growing requirement for accuracy in cylindrical features, straightness and parallelism also become major tolerances affecting the quality of ground parts. For example, a survey carried out in this work of a diesel engine fuel injector factory revealed that over 80% of plungers did not satisfy the specified cylindricity tolerance and the resultant clearance even when the out of roundness of each measured profile was within the roundness tolerance range. Also, over 95% of them showed that the diameter varied along the axis and a bell-mouthed shape was generated after centerless through-feed grinding.

During centerless through-feed grinding, the length of the contact line and the magnitude of the grinding force, which acts between the grinding

* **E-mail** : kangkim@kookmin.ac.kr
TEL : +82-2-910-4676; **FAX** : +82-2-910-4839
School of Mechanical and Automotive Engineering, Kookmin University, 861-1 Jungreung-dong, Sungbook-gu, Seoul 136-702, Korea. (Manuscript **Received** February 3, 2003; **Revised** April 14, 2003)

wheel and the previous and/or following workpieces, vary with every change of the axial location of the current workpiece. Hence, a new coordinate system, variable stages of grinding procedure, a grinding force curve of previous and/or following workpieces, and a global deflection concept are introduced to treat the axial motion of the workpiece during this process.

The objectives of this research are to develop a model which include the effect of the axial movement of workpieces on the form generation mechanism and to investigate the effects of the major grinding variables in a centerless through-feed grinding process through experiments and simulations. One of these grinding variables is the center height angle that has been known as the most important variable in the 2-D rounding mechanism (Yonetsu, 1959a, 1959b; Rowe and Barash, 1964; Rowe et al., 1965). The other variables are the regulating wheel tilt angle and the grinding wheel surface shape. By these variables, the total number of workpiece rotations and the amount of material removal per unit workpiece rotation are changed. For the experiments, two types of specimens were prepared. The first type was a perfectly cylindrical shape and the second type was a cylindrical shape with a flat. The computer simulations were also carried out to verify this model.

2. Grinding Geometry and Coordinate System

The through-feed grinding is performed by passing the workpiece between the grinding wheel and the regulating wheel. The workpiece undergoes radial and axial movements as shown in Fig. 1. To generate axial motion of the workpiece along the line of contact with the grinding wheel, the regulating wheel is tilted with respect to the workpiece axis and has a hyperboloid ruled surface (Yonetsu, 1960). The axial movement rate is approximated by multiplying the diameter of the regulating wheel by π, the angular velocity, and the sine of the tilt angle, φ (SME, 1983). The change of the angle, τ, between the regulating

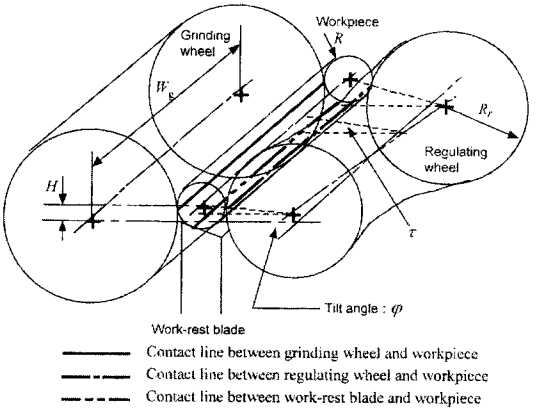

Fig. 1 Schematic diagram of through-feed grinding

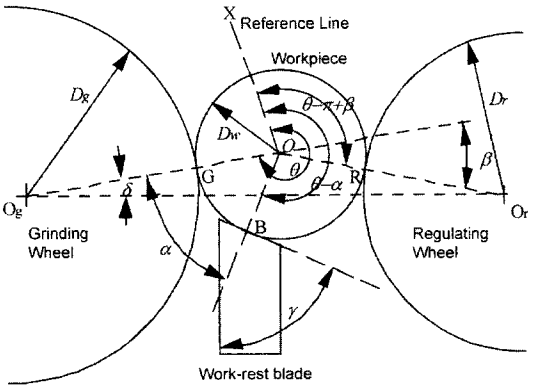

Fig. 2 Centerless grinding geometry

wheel contact normal and the horizontal line is somewhat larger, but the workpiece center height angle, β, is kept the same in the workpiece. Therefore, variation of τ has no effect on β.

Also, Fig. 2 shows the simplified 2-D configuration of the centerless grinding geometry where θ is the angle of rotation ($\angle O_gOX$) between the initial reference line OX on the work-piece and the grinding wheel contact normal shown as OO_g. In Fig. 2, α is the angle ($\angle O_gOB$) between the line OO_g and the normal line OB of the work-rest blade surface, β is the supplementary angle ($\pi-\angle O_gOO_r$) between the line OO_r connecting the work-piece center and the regulating wheel center and the line OO_g, and γ is the top angle of the work-rest blade. The reference line OX coincides with the line OO_g at the beginning of grinding.

Figure 3 shows the coordinate system for the through-feed grinding process where z is the axial

distance from the leading end of the workpiece to the simulation layer. In Fig. 3, S is the axial distance from the initial workpiece contact point

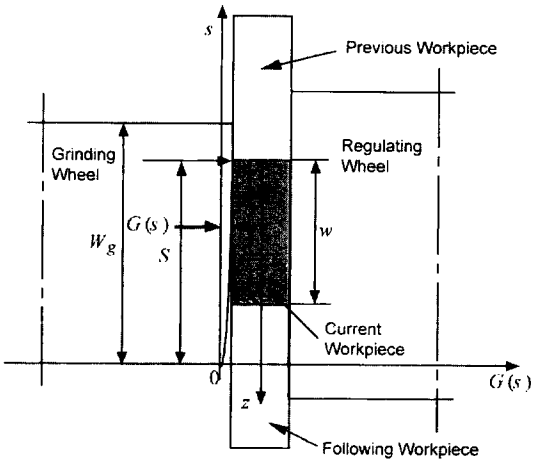

Fig. 3 Coordinate system for through-feed grinding

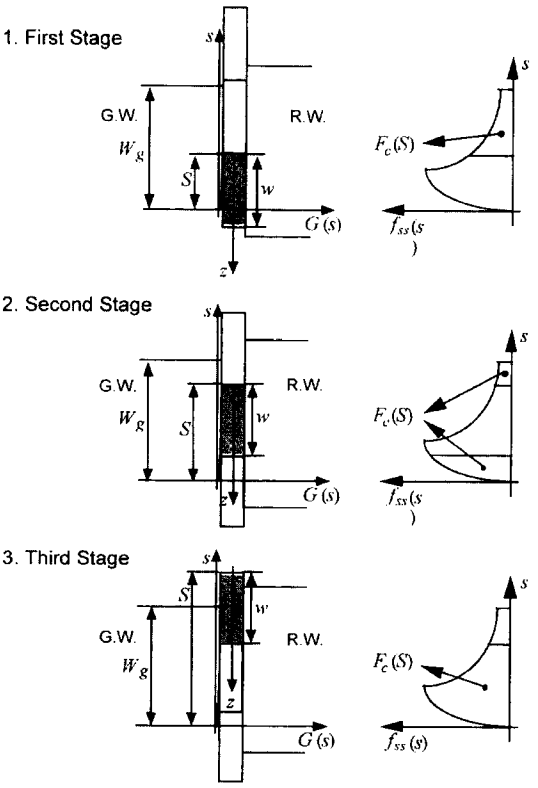

Fig. 4 Procedure of through-feed grinding and grinding force of previous and/or following workpieces

of the grinding wheel to the leading end of the workpiece and s is the axial distance from the initial workpiece contact point of the grinding wheel to a certain grinding wheel contact point. To make the axial motion of the workpiece easy at the initial stage of the through-feed process, the grinding wheel has a crown of which the surface is expressed as $G(s)$.

This process is composed of three stages as shown in Fig. 4. The first stage starts just after the leading end of the workpiece contacts the wheels and finishes when the full width of the workpiece is in contact with both wheels. The second stage starts right after the first stage and finishes when the leading end of workpiece leaves the grinding wheel. The third stage also starts just after the second stage and finishes when the trailing end of the workpiece leaves the grinding wheel.

3. Grinding Force of Previous and/or Following Workpieces

During through-feed grinding, the workpieces are fed to a centerless grinding machine continuously. After a certain period from the start of the grinding process, the space between the wheels is filled with a series of workpieces. Therefore, to understand the centerless through-feed grinding process, all the workpieces which are under grinding at the same time must be considered simultaneously. There are two methods to do this. The first method considers all the surface data of the workpieces that are engaged between the wheels at the same time, and the second method considers the effect of the previous and/or following workpieces on the current workpiece. The model which is uses the first method will be more accurate, but it is difficult and unrealistic compared with the actual production line. So even though the second approach requires more ideal assumptions, it is a feasible approach.

If the variation in the workpiece external shape is small, the through-feed grinding process can be regarded as a semi-steady state. Thus, the normal grinding force distribution along the grinding wheel axis can be assumed as a semi-steady curve, $f_{ss}(s)$. From the grinding wheel shape function,

$G(s)$, and the regulating wheel tilt angle, φ, the equivalent infeed grinding condition (infeed rate and number of workpiece rotations) is derived. The imaginary workpiece length for the equivalent infeed grinding process is also equal to the axial displacement of the current workpiece during one revolution of this current workpiece. To be feasible for any possible shape of a workpiece, $f_{ss}(s)$ must be found under the worst case situation. The worst case $f_{ss}(s)$ corresponds to the maximum force curve which is generated when this imaginary workpiece is a perfect cylinder. Using the 2-D infeed model, if it is assumed that this imaginary workpiece is ground under this equivalent infeed grinding condition, $f_{ss}(s)$ can be found easily. Therefore, the force, $F_c(S)$, which is applied to the machine system by the previous and/or following workpieces when the leading end of the current workpiece reaches S, is defined as

$$F_c(S)=\int_0^a f_{ss}(s)\,ds+\int_b^{W_g} f_{ss}(s)\,ds \quad \begin{pmatrix} \text{if } S-w>0 & a=S-w, & \text{if } S-w\le 0 & a=0 \\ \text{if } S<W_g & b=S, & \text{if } S\ge W_g & b=0 \end{pmatrix} \tag{1}$$

where W_g is the width of grinding wheel and w is the length of the workpiece.

4. Global Deflection and Effective Apparent Depth of Cut

$F_c(S)$ causes an elastic deflection of the machine system. It is assumed that this global deflection increases the distance between the wheels constantly along the axis of the grinding wheel. The amount of this global deflection, $D_c(S)$, when the leading end of this workpiece reaches S, is expressed as

$$D_c(S)=\frac{F_c(S)}{K_e} \tag{2}$$

where K_e is the elasticity factor.

The total grinding force, $F_n(S)$, is exactly equal to the total deflection force. The deflection force of each layer is approximated by multiplying the deflection, which is equal to the difference between the maximum apparent depth of cut, $D(\theta,\ \eta_{\max},\ z_i)$, and the maximum true depth of cut, $L(\theta,\ \eta_{\max},\ z_i)$, by the elasticity factor. $F_n(S)$ is also expressed as the sum of $F_c(S)$ and the normal grinding force, which causes material removal of the current workpiece, $F_o(S)$. If the number of layers of the current workpiece which are engaged in the grinding wheel is l_e, and K_e is regarded as a parallel connection of K_e/l_e,

$$\begin{aligned} F_o(S)&=F_n(S)-F_c(S) \\ &\cong\frac{K_e}{l_e}\Big[\sum_{\text{for all G.W. contact layers}}\{D(\theta,\ \eta_{\max},\ z_i)-L(\theta,\ \eta_{\max},\ z_i)\}\Big]-F_c(S) \\ &=\frac{K_e}{l_e}\Big[\sum_{\text{for all G.W. contact layers}}\Big\{D(\theta,\ \eta_{\max},\ z_i)-\frac{F_c(S)}{K_e}\Big\}-L(\theta,\ \eta_{\max},\ z_i)\Big] \\ &=\frac{K_e}{l_e}\Big[\sum_{\text{for all G.W. contact layers}}\{D(\theta,\ \eta_{\max},\ z_i)-D_c(S)\}-L(\theta,\ \eta_{\max},\ z_i)\Big] \end{aligned} \tag{3}$$

where

$$S=R\theta\sin\varphi \tag{4}$$

If the effective apparent depth of cut, $D_e(\theta,\ \eta,\ z_i)$, is defined as

$$D_e(\theta,\ \eta,\ z_i)=D(\theta,\ \eta,\ z_i)-D_c(S) \tag{5}$$

the normal grinding force acting on the current workpiece, $F_o(S)$, can be expressed as

$$F_o(S)=\frac{K_e}{l_e}\Big[\sum_{\text{for all G.W. contact layers}}\{D_e(\theta,\ \eta_{\max},\ z_i)-L(\theta,\ \eta_{\max},\ z_i)\}\Big] \tag{6}$$

Therefore, the centerless through-feed grinding process is decomposed as a grinding process of the previous and/or following workpieces and a

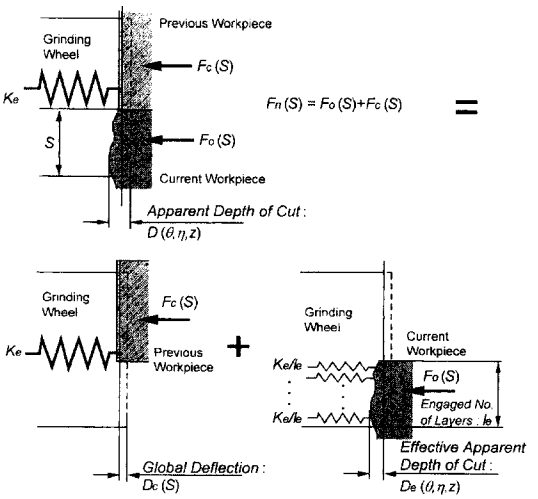

Fig. 5 Global deflection and effective apparent depth of cut

grinding process of the current workpiece. This is shown in Fig. 5. If only a single workpiece is engaged between the wheels at the same time and the force, $F_o(S)$, is applied to the machine system while this workpiece is passing between the wheels, the apparent depth of cut of the current workpiece is reduced by $D_c(S)$, because of $F_c(S)$. Thus, the continuous through-feed grinding process can be regarded as this discrete through-feed grinding process by introducing the concept of the effective apparent depth of cut regardless of the exact external shape of the previous and/or following workpieces.

5. Experiment and Simulation

The pre-grinding shapes of the specimens in this experiment were cylindrical hollow bar shapes with and without a flat along the axis as shown in Fig. 6. The material of the specimens was a hardened steel with Rockwell C hardness of 62-63. The diameter deviation, roundness error, straightness, and taper of the pre-grinding specimens, except the flat area, were within 2 μm, and the deviation of flat depth was within 4 μm.

In a through-feed process, if the regulating wheel speed is fixed, the total number of workpiece rotations is determined by the regulating wheel tilt angle and the feed rate. The number of rotations for the feed are also governed by the grinding wheel surface shape, which is formed by a dressing template. Therefore, the center height angle, β, the regulating wheel tilt angle, and the shape of grinding wheel dressing template were selected as control variables for the experiments. The through-feed experiments are also grouped into three parts. During the first experiment, β was changed from 2° to 8° at intervals of 2°. The second experiment was performed under three different tilt angles (2°, 3°, and 4°). For the final experiment, two types of grinding wheel dressing templates, which have different inlet slopes and ratios between the inlet crown length and flat length, were prepared. The experimental conditions are presented in Table 1.

To investigate the ground specimens 3-dimensionally, nine measuring layers (from 0 to 8) of each specimen were selected as shown in Fig. 6. Even though a cylindricity profile can be drawn, it is insufficient to reveal the 3-D shape of the ground specimen because it only shows the relative peripheral data from an unknown reference circle. To compensate for this problem, diameters were measured with cylindricity profiles. The cylindricity profiles and the diameters were measured on the Talyrond 252 machine from Rank Taylor Hobson Co. and the Zygo LTS bench micrometer series 1200 machine from Zygo Co., respectively. If a diameter is measured between two points around where waviness variations of the roundness profile are minimized, the possible measurement error can be reduced. In case of the

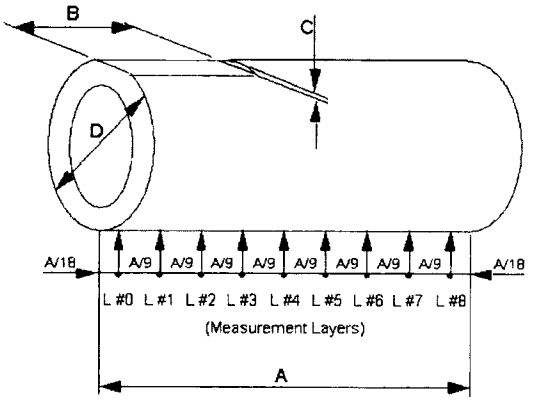

(unit: mm)

Type	A (±0.3)	B	C (±0.004)	D (±0.002)
T0	74	0	0.05	23.534
T1		74		

Fig. 6 Details of the specimen geometry

Table 1 Grinding conditions

Grinding Machine	Cincinnati CINCO 15
Grinding Wheel	97A80J6VFM ϕ542.7×101.6×304.8 mm hole
Regulating Wheel	A80R2 ϕ302.2×101.6×127.0 mm hole
Work-rest Blade	Sintered Carbide (γ=60°)
Center Height Angle (β)	4°
R.W.Speed	30 rpm
G.W.Speed	1200 rpm
Dressing Traverse Rate	80 μm/rev
Infeed Rate	1.1 μm/rev
No. of Infeed Rev.	42 rev
No. of Spark-out Rev.	39 rev

specimens with a flat, two points which have $\pm 90°$ difference from the middle point of the flat were selected as the measuring points at each layer.

The computer simulations were carried out using the previously developed 3-D centerless through-feed grinding model. Each simulation was carried out under the corresponding experimental condition. The threshold grinding force of 210 N was quoted from the reference (ASM International, 1989) and the machining factor was calculated as 240MN/m (Kim et al., 1992). The elasticity factor of 24 MN/m was cited from the reference (Reshetov and Portman, 1988).

6. Discussion

6.1 Grinding force of previous and/or following workpieces and global deflection

Figure 7 shows the distributions of this force under the experimental conditions. This figure shows that the force curve of a high tilt angle has larger values than that of a low tilt angle, but the higher tilt angle means higher axial speed. Thus, there are no significant differences in the total forces between the different grinding conditions. From this, the correctness of this force distribution curve is proved indirectly because the total grinding force applied to the workpiece is independent of the grinding cycle if there is no significant difference in the total amount of material removal.

$F_c(S)$, which is calculated using Eq. (1), is also shown in Fig. 8. $F_c(S)$ is a 'V' shape force function. Accordingly, the total grinding force of the previous and/or following workpieces, which is applied to a certain layer, z_i, of the current workpiece while it is engaged between the wheels, varies depending on the relative position of the leading end of current workpiece. In this case, the total grinding force, which is applied around the middle of the current workpiece by the previous and/or following workpieces, is smaller than the total force which affects each end of it. Therefore, when the middle of the current workpiece is ground, there exists relatively small global deflection of the grinding wheel compared with each

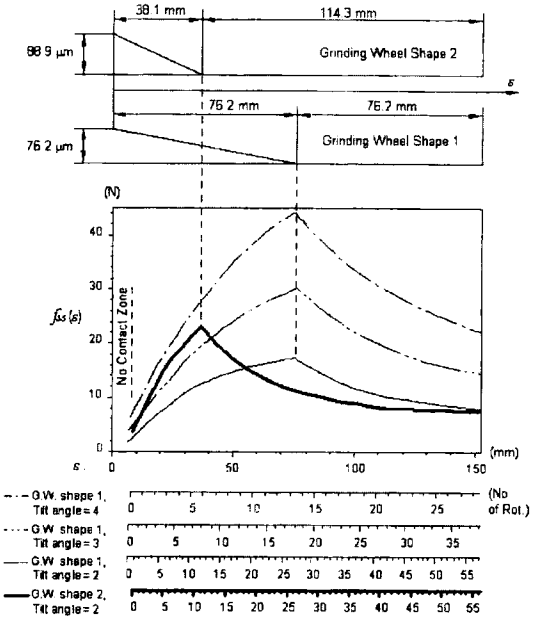

Fig. 7 Grinding force distribution along the grinding wheel axis in through-feed grinding

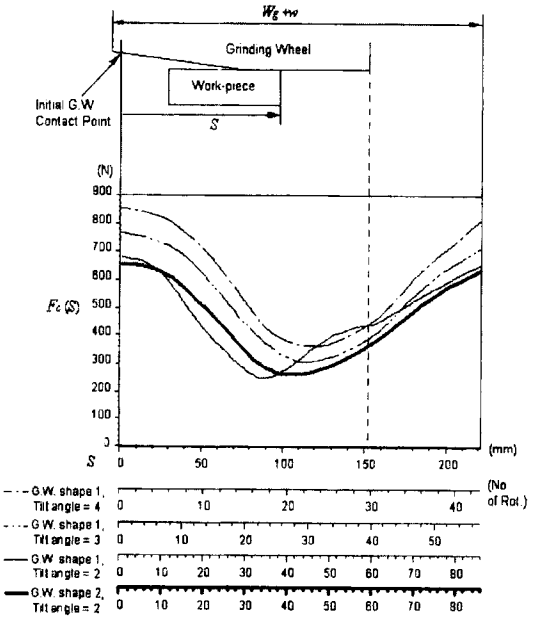

Fig. 8 Grinding force of previous and/or following workpieces in continuous through-feed grinding

end. Accordingly, the middle of the workpiece experiences more material removal. As a result, the ground workpiece has a bell-mouthed shape.

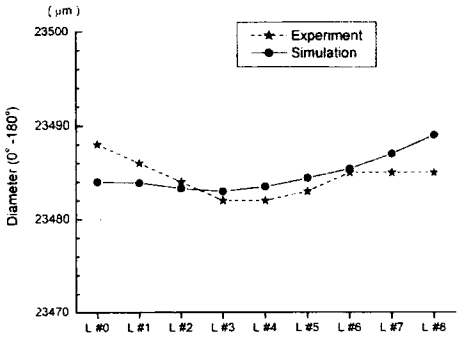

(a) β=2°, R.W. Tilt Angle=3°, G.W. Shape 1

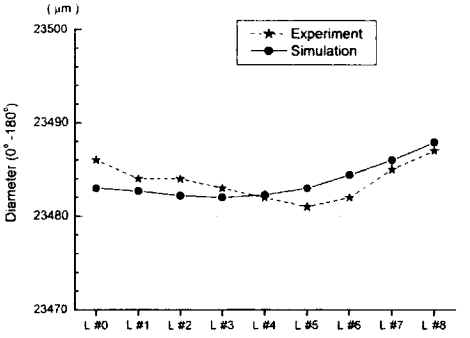

(b) β=4°, R.W. Tilt Angle=3°, G.W. Shape 1

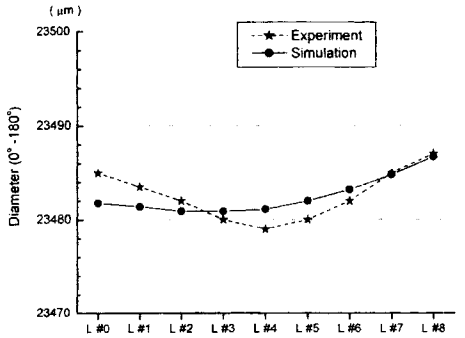

(c) β=6°, R.W. Tilt Angle=3°, G.W. Shape 1

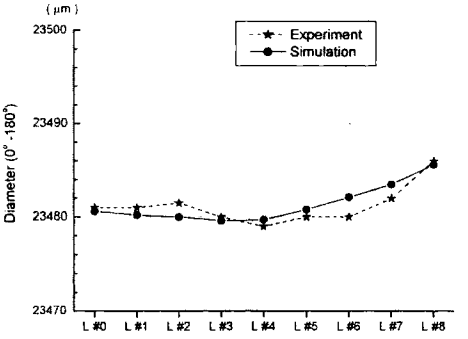

(d) β=8°, R.W. Tilt Angle=3°, G.W. Shape 1

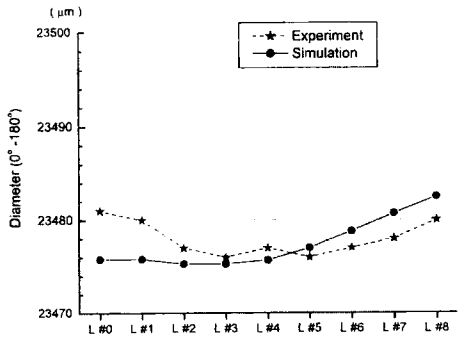

(e) β=6°, R.W. Tilt Angle=2°, G.W. Shape 1

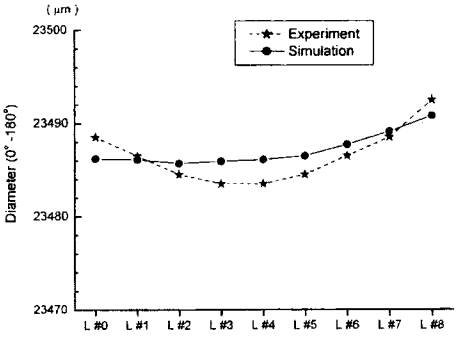

(f) β=6°, R.W. Tilt Angle=4°, G.W. Shape 1

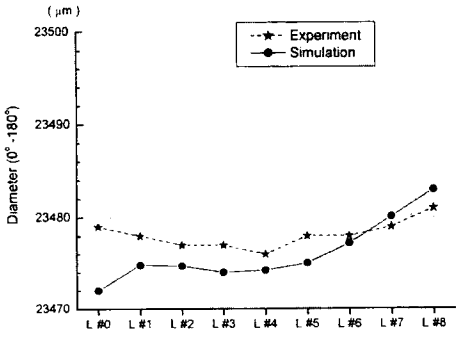

(g) β=6°, R.W. Tilt Angle=2°, G.W. Shape 2

Fig. 9 Variation af diameter along the specimen axis. (specimen type : T0)

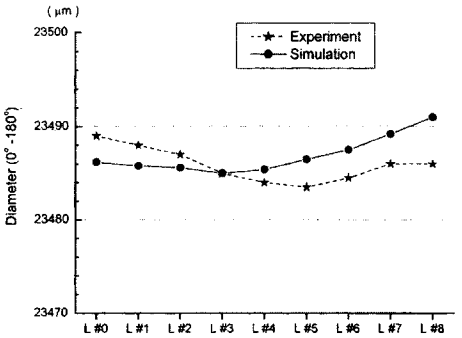

(a) β=2°, R.W. Tilt Angle=3°, G.W. Shape 1

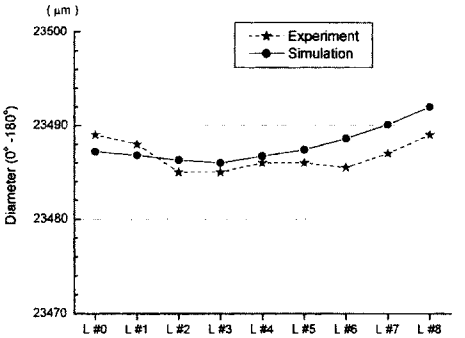

(b) β=4°, R.W. Tilt Angle=3°, G.W. Shape 1

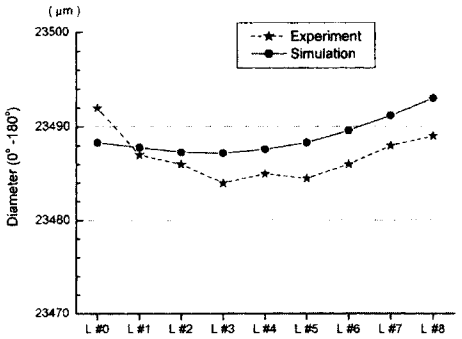

(c) β=6°, R.W. Tilt Angle=3°, G.W. Shape 1

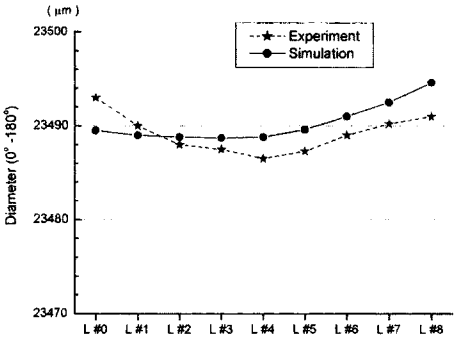

(d) β=8°, R.W. Tilt Angle=3°, G.W. Shape 1

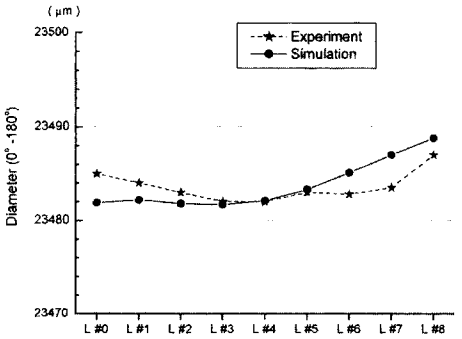

(e) β=6°, R.W. Tilt Angle=2°, G.W. Shape 1

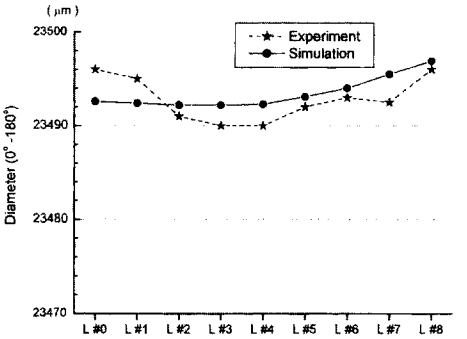

(f) β=6°, R.W. Tilt Angle=4°, G.W. Shape 1

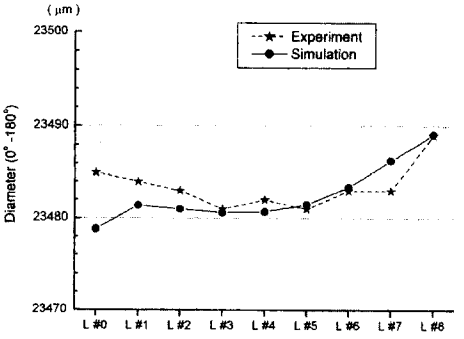

(g) β=6°, R.W. Tilt Angle=2°, G.W. Shape 2

Fig. 10 Variation af diameter along the specimen axis. (specimen type : T1)

6.2 Effects of grinding variables

Figure 9 and 10 show the variation of diameter along the specimen axis when the specimens were T0 and T1, respectively. The measured diameters and the simulated diameters are compared in each figure. Most figures reveal that the minimum diameters are located around the middle of the specimens and the diameters are gradually increased toward both ends.

When the center height angle, β, was changed, it was hard to find any difference between the results in Figs. 9(a)-(d) and 10(a)-(d). From this, it is supposed that β has no relation with the variation of diameter even though it has been known as the most important variable for the roundness control of the centerless ground parts.

If the regulating wheel tilt angle, φ, is increased, the total number of rotations of the workpiece is decreased and the total material removal is also decreased. Accordingly, the corresponding figures (Figs. 9(e), (c), (f) and 10 (e), (c), (f)) show that the overall diameters are increased by increasing φ. It is not easy to find any relation between φ and the variation of diameter from the measured data. However, the simulation results imply that there is less variation in diameter when φ is increased.

The effect of the grinding wheel shape is shown in Figs. 9(e), (g) and 10(e), (g). Depending on this shape, material removal rate is changed. Type 2 grinding wheel dressing template was designed to make the inlet crown slope of the grinding wheel steeper compared with Type 1. Through this experiment and simulation, it was revealed that steeper inlet crown generates worse tapering characteristic. This tendency is found more clearly in the simulation result.

6.3 Simulation error analysis

The through-feed simulation results show a somewhat large error range. Except for the experimental, measurement, and computation errors, the through-feed model has two important error factors in itself. One is caused by the modeling of grinding force of the previous and/or following workpiece, $F_c(S)$, and the other is caused by the assumption of global deflection of the grinding wheel.

$F_c(S)$ was introduced to compensate for the effect of the other workpieces that are engaged between the wheels and the current workpiece simultaneously. In this situation, because only the current workpiece shape is known, the geometry of other workpieces must be assumed as a perfectly cylindrical shape. Thus, the real grinding force acting on the current workpiece may be larger than the simulated grinding force. This is one of the reasons for the simulation error.

During a real grinding process, the grinding wheel is deflected not only locally but also globally. The local deflection occurs at the workpiece contact region and the global deflection occurs in the machine system. However, it is very difficult to separate the global deflection from the machine system deflection. Besides, there is no unified standard or method that is related to the machine elasticity. In this model, the global deflection concept was added to the local deflection concept under the parallel deflection assumption to relate the effect of $F_c(S)$ to the apparent depth of cut of the current workpiece. As a result, in this case, the errors of two different deflections were superposed. This is the other reason for the simulation error in the 3-D through-feed model.

7. Conclusion

The objectives of this research were to develop a model of the axial movement of parts and to investigate the effects of the major grinding variables on the shape of ground parts in a centerless through-feed grinding process. By introducing the grinding force curve of previous and/or following workpieces and a global deflection concept, bell-mouthed shape generation during this process was explained theoretically. Through experiments and simulations it was found that the major grinding variables, which have an effect on this bell-mouthed shape, are the regulating wheel tilt angle and the grinding wheel inlet shape. Also, it was revealed that the center height angle has no relation with this shape.

References

ASM International, 1989, *Metals Handbook, 9th Edition, Vol. 16 Machining*, pp. 422, 448.

Dall, A. H., 1946, "Rounding Effect in Centerless Grinding," *Mechanical Engineering*, Vol. 68, No. 4, ASME, pp. 325~329.

Kim, K., Chu, C. N. and Barash, M. M., 1992, "Roundness Generation during Centerless Infeed Grinding," *Transactions of NAMRI of SME*, 20, pp. 167~172.

Meis, F. U., 1980, *Geometrische und kinematische Grundlagen fur das spitzenlowe Durchlaufschleifen*, Ph. D. Dissertation, T. H. Aachen, W. Germany.

Reshetov, D. N. and Portman, V. T, 1988, *Accuracy of Machine Tools*, ASME Press, p. 275.

Rowe, W. B. and Barash, M. M., 1964, "Computer Method for Investigating the Inherent Accuracy of Centerless Grinding," *Int. J. Mach. Tool Des. Res.*, Vol. 4, pp. 91~116.

Rowe, W. B., Barash, M. M. and Koenigsberger, F., 1965, "Some Roundness Characteristics of Centerless Grinding," *Int. J. Mach. Tool Des. Res.*, Vol. 5, pp. 203~215.

SME, 1983, *Tool and Manufacturing Engineers Handbook 4th ed., Vol. 1, Machining*.

Yonetsu, S., 1959a, "Consideration of Centerless Grinding Characteristics Through Harmonic Analysis of Out-of-Roundness Curve," *Proc. Fujihara Memorial Faculty of Engineering*, Keio Univ., Vol. 12, No. 47, pp. 8~26.

Yonetsu, S., 1959a, "Forming Mechanism of Cylindrical Work in Centerless Grinding," *Proc. Fujihara Memorial Faculty of Engineering*, Keio Univ., Vol. 12, No. 47, pp. 27~45.

Yonetsu, S., 1960, "Consideration on the Control Wheel Truing of a Centerless Grinder," *Proc. Fujihara Memorial Faculty of Engineering*, Keio Univ., Vol. 13, No. 49, pp. 1~9.